Physics – Uspekhi **42** (3) 245 – 260 (1999)

REVIEWS OF TOPICAL PROBLEMS PACS numbers: **02.40.–k**, **36.20.–r**, 43.25.Rq, 87.15.He

Nonlinear dynamics of zigzag molecular chains

A V Savin, L I Manevich¶, P L Christiansen, A V Zolotaryuk

Contents

Abstract. Nonlinear, collective, soliton type excitations in zigzag molecular chains are analyzed. It is shown that the nonlinear dynamics of a chain dramatically changes in passing from the one-dimensional linear chain to the more realistic planar zigzag model — due, in particular, to the geometry-dependent anharmonism that comes into the picture. The existence or otherwise of solitons is determined in this case by the interplay between the geometrical anharmonism and the physical anharmonism of the interstitial interaction, of opposite signs. The nonlinear dynamic analysis of the three most typical zigzag models (two-dimensional alpha-spiral, polyethylene transzigzag backbone, and the zigzag chain of hydrogen bonds) shows that the zigzag structure essentially limits the soliton dynamics to finite, relatively narrow, supersonic soliton velocity intervals and may also result in that several acoustic soliton types (such as extension and compression varieties) develop simultaneously in the chain. Accordingly, the inclusion of chain geometry is necessary if physical phenomena are to be described in terms of solitary waves.

¶ The author is also known by the name L I Manevitch. The name used here is a transliteration under the BSI/ANSI scheme adopted by this journal.

A V Savin State Institute for Problems of Physics and Technology, ul. Prechistenka 13/7, 119034 Moscow, Russia
Tel. (7-095) 248 81 59. Fax (7-095) 201 24 94
E-mail: asavin@center.chph.ras.ru; alex@savin.msk.ru
L I Manevich N N Semenov Institute of Chemical Physics, Russian Academy of Sciences, ul. Kosygina 4, 117977 Moscow, Russia
Tel. (7-095) 939 75 15. Fax (7-095) 137 82 84
E-mail: lmanev@center.chph.ras.ru
P L Christiansen Department of Mathematical Modelling, Technical University of Denmark, DK-280 Lyngby, Denmark
Tel. 45-4588 1433. Fax 45-4593 1235
E-mail: plc@imm.dtu.dk
A V Zolotaryuk N N Bogolyubov Institute for Theoretical Physics, National Academy of Sciences of Ukraine, 252143 Kiev, Ukraine
Tel. (380-44) 266 09 43. Fax (380-44) 266 59 98
E-mail: azolo@gluk.apc.org

Received 4 June 1998, revised 24 October 1998
Uspekhi Fizicheskikh Nauk **169** (3) 255 – 270 (1999)
Translated by A S Dobroslavskiĭ; edited by A Radzig

1. Introduction

Advances in contemporary nonlinear physics have led to the discovery of new elementary mechanisms that determine on the molecular level the progression of many physical processes in crystals and other ordered molecular structures. Today the role of acoustic solitons is quite clear to ensure the most efficient mechanism of energy transfer in such processes, for example, as heat conduction and breakdown of solids [1 – 4], or propagation of signals in biological macromolecules [5]. Topological solitons serve as models of structural defects in polymer crystals, and their mobility ensures the possibility of such processes as plastic deformation [6 – 8], relaxation [9], premelting [10]. The role of topological solitons in the description of structural transitions and chemical reactions was discussed in Refs [11 – 14].

Early theoretical investigations of the nonlinear dynamics of macromolecular chains [15 – 18] considered one-dimensional (spatially linear) models with the positive-sign anharmonism, which only took into account the longitudinal displacements of atoms (molecules) in the chain. In this case, the repulsion between the approaching adjacent sites in the chain grows faster than in the harmonic approximation. One of the consequences of this fact is the existence of dynamically

stable solitary compression waves, which are supersonic acoustic solitons.

For the first time the effects of transverse vibrations of molecules in the chain on the dynamics of solitons were analyzed in Ref. [19]. The solitons were found to be highly sensitive to transverse perturbations. This issue is studied in greater detail in Refs [20 – 24].

Without taking the transverse movement of units of the chain into account it would be impossible to understand the mechanism of functioning of certain biomolecular chains. In a DNA molecule, for example, the opening of pairs of bases in the transverse direction ensures the possibility of denaturation. The Peyrard – Bishop model of melting of DNA [25 – 27] only takes into account the transverse motion of conjugate pairs of bases. Even though an isolated DNA molecule is considered (which has both longitudinal and transverse degrees of freedom), this model in fact describes the one-dimensional dynamics of a molecular chain on an effective substrate. A comprehensive review of the models of nonlinear DNA dynamics can be found in the monograph [28].

The real geometry of biomolecular systems calls for the development of two- and three-dimensional models. This is the only way of taking into consideration the anharmonism of the system vibrations caused by its geometry. For example, for the simplest cluster model of enzyme protein α-chymotrypsin it was shown that geometrical anharmonism in a two-dimensional system ensures transfer of energy between the degrees of freedom even in the case of small amplitudes [29, 30].

Application of the latter-day computational capabilities to the analysis of nonlinear dynamics of molecular systems permits going over from simple one-dimensional models to the more sophisticated two- and three-dimensional models that better represent the actual geometric structure of the system. The most coherent and convenient objects in this respect are zigzag molecular chains.

In this paper we consider the planar (two-dimensional) dynamics of a free molecular chain. Obviously, the chain in the absence of a substrate will only have a ground state with a regular stable structure provided that the interaction between remote neighbours is taken into account in addition to the short-range interaction. The inclusion of long-range interaction results in that the chain displays a *secondary structure*, such as is often encountered in many macromolecules (DNA, proteins, and the like). Geometrically, the secondary structure takes on the shape of a spiral, the flat zigzag being a particular such case.

If we only consider the longitudinal and transverse displacements, the model of the spiral will become much simpler and will reduce essentially to a *two-dimensional spiral* (flat zigzag chain). Here, the primary structure results from the interaction between first neighbours, and the secondary from that between second neighbours. Such a system [31] may be regarded as the simplest theoretical model of an isolated biomolecular chain. For the alpha-spiral of protein, for example, the interaction between the closest neighbours involves deformations of the relatively rigid valence bonds, and interaction with second neighbours involves deformations of the soft hydrogen bonds.

The flat zigzag structure is much closer to reality than the one-dimensional anharmonic lattice. Observe that the passage from two- to three-dimensional models in the description of certain important types of dynamic behaviour does not bring about any significant modifications [31, 32]. At the same time, as pointed out in Refs [19 – 22], the distinction between one- and two-dimensional models is fundamental.

Even in a one-dimensional model the inclusion of the interaction with second neighbours [33, 34] dramatically changes the dynamics of the system. In a two dimensional model this gives rise to a secondary structure, which brings a new factor into the dynamics of the system: *geometrical anharmonism*. Even if all the molecules are bound with harmonic forces, the geometry of the system gives rise to an effective negative anharmonism. This effect was first studied in Ref. [35] in connection with the breather-like solutions of the dynamic equations of one-dimensional chain in three-dimensional space.

Many polymer macromolecules have a flat zigzag shape. For example, the polyethylene (PE) macromolecule in three dimensions has a stable two-dimensional *transzigzag* conformation. Here, the interaction with the first neighbours takes place through deformation of valence bonds, and that with the second and third neighbours occurs through the deformation of valence and torsion angles. As shown in Refs [36, 37], in the approximation of infinitely rigid valence bonds the transition from the rectilinear chain to the transzigzag conformation leads to a dramatic change in the type of soliton solutions. Instead of compression solitons, the nonlinear elementary excitations come to be represented by extension solitons that owe their existence to the geometric anharmonism.

The flat zigzag shape is also featured by chains of hydrogen bonds $\cdots H-X\cdots H-X\cdots H-X\cdots$ in hydrogen halides [38 – 40], where X are fluorine, chlorine, bromine, and iodine, respectively. Here, the zigzag structure of the chain is due to the orientation interaction between adjacent molecules.

The purpose of this paper is to give a classification of soliton excitations in zigzag molecular chains, and to analyze the conditions of their existence and stability.

Section 2 deals with the study of nonlinear dynamics based on the model of a two-dimensional spiral — a flat zigzag with the interaction of the first and second neighbours. The dynamic properties of compression solitons are studied.

In Section 3 we present the results of the study of dynamics of extension solitons in the PE molecule in the context of a realistic model that takes into account deformation of both the valence angles and valent bonds.

In Section 4 we discuss the results of the study of nonlinear dynamics of flat zigzag chains of hydrogen bonds.

The main results of this paper are summarized in the Conclusions. The Appendices give a brief description of numerical techniques used for finding the soliton solutions.

2. Solitons in the molecular chain with secondary structure

Here we are going to consider the simplest two-dimensional model of an alpha-spiral protein macromolecule [31]. Deformations of valence bonds in this model are taken into account via the interactions between first neighbours, and deformations of hydrogen bonds linking the peptide groups are taken into account via the interactions between second neighbours. These interactions are assumed to exhibit central symmetry. We shall perform a detailed 'soliton' analysis of the model, outline the classification of soliton solutions, and check their stability by numerical simulation of dynamic behaviour.

2.1 Generalized model of a zigzag chain

Consider a planar zigzag chain represented schematically in Fig. 1a. Let the zigzag of the chain be directed along the x axis, and lie in the xy plane; then at equilibrium the nth chain molecule has the coordinates

$$x_n^0 = nl_x\,, \qquad y_n^0 = \frac{(-1)^n l_y}{2}\,,$$

where l_x and l_y are the longitudinal and the transverse steps of the zigzag, respectively. Our chain is a two-dimensional spiral. It may be regarded as two parallel linear chains with a period $l = 2l_x$, linked together by a zigzag chain of rigid (valent) bonds. The geometry of the chain is completely determined by the step l and the angle of the zigzag $\alpha = 2\arctan(l_x/l_y)$.

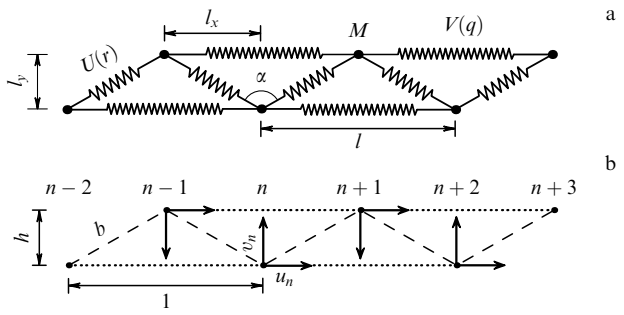

Figure 1. (a) Model of a zigzag-shaped molecular chain, and (b) the local coordinate systems u_n, v_n. Zigzag angle $\alpha = 2\pi/3$.

Now it is convenient to go over from the absolute coordinates of the nth molecule x_n, y_n to the dimensionless relative variables

$$u_n = \frac{x_n - x_n^0}{l}\,, \qquad v_n = \frac{(-1)^{n+1}(y_n - y_n^0)}{l}\,.$$

Here u_n and v_n define, respectively, the dimensionless longitudinal and transverse displacements of the nth molecule from its equilibrium position, the positive direction of the transverse displacement being towards the centre of the zigzag of the chain (Fig. 1b). Then the dimensionless equilibrium length of the rigid bond is $b = (h^2 + 1/4)^{1/2}$, where $h = l_y/2l_x = (1/2)\cot(\alpha/2)$ is the dimensionless parameter of the zigzag width.

The Hamiltonian of the chain may be expressed as

$$H = \sum_n \left\{ \frac{1}{2} Ml^2(\dot{u}_n^2 + \dot{v}_n^2) + Kl^2\big[U(r_n) + V(q_n)\big] \right\}, \qquad (1)$$

where M is the mass of each molecule of the chain, K is the characteristic rigidity coefficient, and a dot above the symbol denotes differentiation with respect to time t. The dimensionless potentials of intermolecular interaction $U(r)$ and $V(q)$ describe interaction between first and second neighbours (Fig. 1a). For a two-dimensional model of the alpha-spiral, M corresponds to the mass of the peptide group, $U(r)$ to the potential of a valent bond, and $V(q)$ to the potential of the hydrogen bond. The dimensionless deformations of the bonds are given by

$$r_n = \sqrt{\left(u_{n+1} - u_n + \frac{1}{2}\right)^2 + (h - v_n - v_{n+1})^2} - b\,,$$

$$q_n = \sqrt{(1 + u_{n+1} - u_{n-1})^2 + (v_{n+1} - v_{n-1})^2} - 1\,.$$

The Hamiltonian (1) corresponds to the set of equations of motion

$$M\ddot{u}_n = -Kl^2 \frac{\partial}{\partial u_n} W_n\,, \qquad M\ddot{v}_n = -Kl^2 \frac{\partial}{\partial v_n} W_n\,, \qquad (2)$$

where

$$W_n = U(r_{n-1}) + U(r_n) + V(q_{n-1}) + V(q_{n+1})\,.$$

To facilitate subsequent manipulations, we introduce the dimensionless time

$$\tau = \omega_0 t\,, \qquad \omega_0 = \sqrt{\frac{K}{M}}\,,$$

and go over from the relative displacements u_n, v_n to the new variables

$$\rho_n = u_{n+1} - u_n\,, \qquad \eta_n = v_n + v_{n+1}\,.$$

We also introduce new notation

$$P_n = \frac{\partial}{\partial \rho_n} U(r_n)\,, \qquad Q_n = \frac{\partial}{\partial \rho_n} V(q_n)\,,$$

$$S_n = \frac{\partial}{\partial \eta_n} U(r_n)\,, \qquad T_n = \frac{\partial}{\partial \eta_n} V(q_n)\,,$$

so that in the new variables we have

$$r_n = \sqrt{\left(\rho_n + \frac{1}{2}\right)^2 + (h - \eta_n)^2} - b\,,$$

$$q_n = \sqrt{(1 + \rho_{n-1} + \rho_n)^2 + (\eta_n - \eta_{n-1})^2} - 1\,.$$

Then the set of equations of motion (2) assumes a more convenient dimensionless form

$$\frac{\mathrm{d}^2\rho_n}{\mathrm{d}\tau^2} = P_{n+1} - 2P_n + P_{n-1} + Q_{n+2} - Q_{n+1} - Q_n + Q_{n-1}\,, \qquad (3)$$

$$\frac{\mathrm{d}^2\eta_n}{\mathrm{d}\tau^2} = -(S_{n-1} + 2S_n + S_{n+1}) + T_{n+1} - T_{n-1} + T_{n+2} - T_n\,, \qquad (4)$$

which was studied in the continuous approximation in Ref. [31].

2.2 Low-amplitude vibrations of the chain

Let us consider the dynamics of low-amplitude waves along the zigzag chain. We use the linear approximation

$$P_n \approx \frac{\kappa_1}{4b^2}(\rho_n - 2h\eta_n)\,, \qquad Q_n \approx \kappa_2(\rho_{n-1} + \rho_n)\,,$$

$$S_n \approx \frac{h\kappa_1}{2b^2}(\rho_n - 2h\eta_n)\,, \qquad T_n \approx 0\,,$$

where

$$\kappa_1 = \left.\frac{\mathrm{d}U}{\mathrm{d}r}\right|_{r=0}, \qquad \kappa_2 = \left.\frac{\mathrm{d}V}{\mathrm{d}q}\right|_{q=0}$$

are the dimensionless rigidities of the interaction potentials. The set of equations of motion (3), (4) is then linearized:

$$\frac{\mathrm{d}^2\rho_n}{\mathrm{d}\tau^2} = \frac{\kappa_1}{4b^2}(\rho_{n+1} - 2\rho_n + \rho_{n+1}) + \kappa_2(\rho_{n+2} - 2\rho_n + \rho_{n-2}) - \frac{h\kappa_1}{2b^2}(\eta_{n+1} - 2\eta_n + \eta_{n-1}), \tag{5}$$

$$\frac{\mathrm{d}^2\eta_n}{\mathrm{d}\tau^2} = \frac{h\kappa_1}{2b^2}(\rho_{n+1} + 2\rho_n + \rho_{n+1}) - \frac{h^2\kappa_1}{b^2}(\eta_{n+1} + 2\eta_n + \eta_{n-1}). \tag{6}$$

We seek solution of the linear set of equations (5), (6) in the form of a harmonic wave

$$\rho_n = A_1 \exp\left(\frac{kn}{2} - \Omega\tau\right), \qquad \eta_n = A_2 \exp\left(\frac{kn}{2} - \Omega\tau\right), \tag{7}$$

where Ω is the circular frequency, and $-2\pi \leqslant k \leqslant 2\pi$ is the dimensionless wave number.

After substitution of expression (7) into the linear set of equations (5), (6) and some straightforward algebra we get the linear dispersion equation

$$\left(\Omega^2 - \frac{\kappa_1}{b^2}\sin^2\frac{k}{4} - 4\kappa_2\sin^2\frac{k}{2}\right)\left(\Omega^2 - \frac{4h^2\kappa_1}{b^2}\cos^2\frac{k}{4}\right) - \left(\frac{h\kappa_1}{b^2}\sin\frac{k}{2}\right)^2 = 0. \tag{8}$$

In the limit of $\kappa_1 \to 0$, when the zigzag splits into two independent linear chains, the dispersion equation (8) reduces to the well-known linear dispersion law for an isolated linear chain:

$$\Omega = 2\sqrt{\kappa_2}\left|\sin\frac{k}{2}\right|.$$

The solution of dispersion equation (8) has two branches:

$$\Omega_\pm^2 = \kappa_1\left[1 + \left(1 - \frac{1}{2b^2}\right)\cos\frac{k}{2}\right] + 2\kappa_2\sin^2\frac{k}{2} \pm \sqrt{\left[\kappa_1\left(1 - \frac{1}{2b^2} + \cos\frac{k}{2}\right) - 2\kappa_2\sin^2\frac{k}{2}\right]^2 + \left(\kappa_1\frac{h}{b^2}\sin\frac{k}{2}\right)^2}.$$

The upper branch $\Omega_+(k)$ corresponds to high-frequency optical phonons, and the lower branch $\Omega_-(k)$ corresponds to low-frequency acoustic phonons. In the long-wave limit ($k \to 0$) the frequency of acoustic phonons is $\Omega_-^2 \to \kappa_2 k^2$, therefore the dimensionless speed of sound in the chain is $v_0 = \sqrt{\kappa_2}$.

The rigidity of the hydrogen bond is approximately one order of magnitude less than that of the valent bond, so for the sake of definiteness we set $\kappa_1 = 1$, $\kappa_2 = 0.1$. We also use the most typical zigzag angle $\alpha = 2\pi/3$. Then the dimensionless width of the zigzag is $h = 1/\sqrt{3} = 0.289$, and the dimensionless length of the valent bond $b = \sqrt{7/12} = 0.577$. The shape of the dispersion curve is shown in Fig. 2. The upper (optical) branch of the curve rises steadily from the minimum value of $\Omega_+(0) = 1$ to the maximum value of $\Omega_+(2\pi) = 1.732$. The lower (acoustic) branch $\Omega_-(k)$ reaches a maximum value of 0.368 at $k = 0.645\pi$. The frequency of acoustic phonons tends to zero at $k \to 0$ and $k \to 2\pi$. These extreme values of the wave number correspond to the long-wave longitudinal and bending waves of the zigzag.

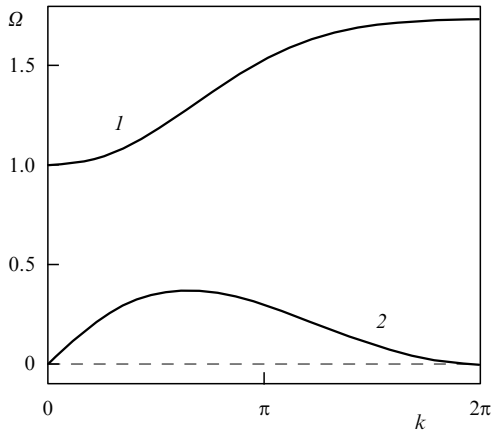

Figure 2. Optical (*1*) and acoustic (*2*) branches of the dispersion curve of a two-dimensional zigzag chain at $k_1 = 1$, $k_2 = 0.1$, and $\alpha = 2\pi/3$.

2.3 Acoustic compression solitons

Now for the description of rigid valent bonds we use the harmonic potential

$$U(r) = \frac{1}{2}\kappa_1 r^2,$$

and the Morse potential for the relatively soft hydrogen bonds:

$$V(q) = \varepsilon\left[\exp(-\beta q) - 1\right]^2 = \kappa_2\left(\frac{1}{2}q^2 - \frac{1}{3}\gamma q^3 + \ldots\right),$$

where $\varepsilon = \kappa_2/2\beta^2$ is the bond energy, $\gamma = 3\beta/2$ the anharmonic constant, and $\beta > 0$ the parameter of the Morse potential. For the sake of definiteness, in future we are going to use fixed values of rigidities $\kappa_1 = 1$, $\kappa_2 = 0.1$, and three characteristic values of the anharmonic constant $\gamma = 1$ ($\beta = 2/3$), $\gamma = 0.1$ ($\beta = 2/30$), and $\gamma = 0.01$ ($\beta = 2/300$) (strong, medium and weak anharmonism).

The acoustic soliton in the zigzag corresponds to the solution of the set of discrete equations (3), (4) in the form of a constant-profile solitary wave

$$\rho_n(\tau) = \rho\left(\frac{n}{2} - v\tau\right), \qquad \eta_n(\tau) = \eta\left(\frac{n}{2} - v\tau\right), \tag{9}$$

where $n = 0, \pm1, \pm2, \ldots$; $\rho(z), \eta(z) \to 0$ at $z \to \pm\infty$, and v is the velocity of the soliton. It is convenient to go over from the absolute velocity v to the relative velocity $s = v/v_0$.

The complexity of the model under consideration and the necessity of taking into account the discrete character of the chain do not allow the shape of the soliton $\rho(z)$, $\eta(z)$ to be found with analytical methods. A high precision calculation of the soliton shape is based on the pseudospectral Eilbeck – Flesch method [41, 42]. Application of this method to the model in question is described in Appendix 6.1. This method allows not only the shape of the soliton solution to be found,

but also its range of existence. Knowing the form of the two-component soliton (9), it is easy to find its dimensionless energy

$$E = \sum_n \left[\frac{1}{2} \left(\frac{\mathrm{d}u_n}{\mathrm{d}\tau} \right)^2 + \frac{1}{2} \left(\frac{\mathrm{d}v_n}{\mathrm{d}\tau} \right)^2 + U(r_n) + V(q_n) \right],$$

the two components of its amplitude $A_\eta = -\eta(0)$, $A_\rho = -\rho(0)$, and the root-mean-square width

$$D = \frac{1}{C} \int_{-\infty}^{\infty} (z - m)^2 \rho(z)\, \mathrm{d}z, \qquad (10)$$

where

$$C = \int_{-\infty}^{\infty} \rho(z)\, \mathrm{d}z, \qquad m = \frac{1}{C} \int_{-\infty}^{\infty} z\rho(z)\, \mathrm{d}z.$$

Numerical analysis indicated that soliton solutions only exist in a finite supersonic interval of velocities $1 < s < s_1$, where s_1 is a certain limiting value of the soliton velocity above which there are no soliton solutions. The width of this interval increases monotonically with the anharmonic constant γ. For example, for the values $\gamma = 0.01$, 0.1, 1 the velocity s_1 is, respectively, 1.03, 1.30, 2.84. The characteristic form of the soliton solution is shown in Fig. 3: the soliton is bell-shaped with respect to both components. In the region of localization of the soliton we observe longitudinal compression and transverse extension of the zigzag of the chain. As the velocity s increases, the energy of the soliton E, the amplitudes of compression A_ρ and extension A_η increase monotonically, and the width of the soliton D monotonically decreases. The particular values of these quantities are given in Table 1. Near the maximum value of the velocity s_1, however, the solution has the form of a soliton against the background of a low-amplitude optical phonon (Fig. 4). The existence of compression solitons is due to the 'physical' anharmonism in the interactions of second neighbours. In addition, the chain features 'geometrical' anharmonism of the opposite sign. As the velocity increases, the amplitude of compression increases, and thus the relative importance of geometrical anharmonism. At $s = s_1$, the physical anharmonism is completely cancelled out by geometrical anharmonism, and the compression solitons no longer exist.

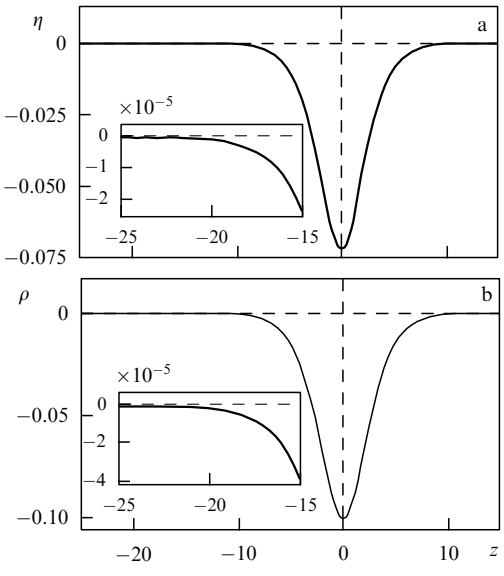

Figure 3. Acoustic compression soliton ($\gamma = 0.1$, $s = 1.05$): (a) soliton profile for transverse displacements; (b) the same for longitudinal displacements.

Table 1. Soliton energy E, amplitudes of longitudinal compression A_ρ and transverse extension A_η, and width D for different values of velocity s ($\gamma = 0.1$).

s	E	A_ρ	A_η	D
1.01	0.00170	0.01487	0.02443	13.06
1.02	0.00478	0.02979	0.04663	9.071
1.03	0.00843	0.04389	0.06595	7.329
1.04	0.01277	0.05807	0.08392	6.284
1.05	0.01763	0.07203	0.10044	5.587
1.06	0.02297	0.08582	0.11571	5.007
1.07	0.02876	0.09941	0.12991	4.457

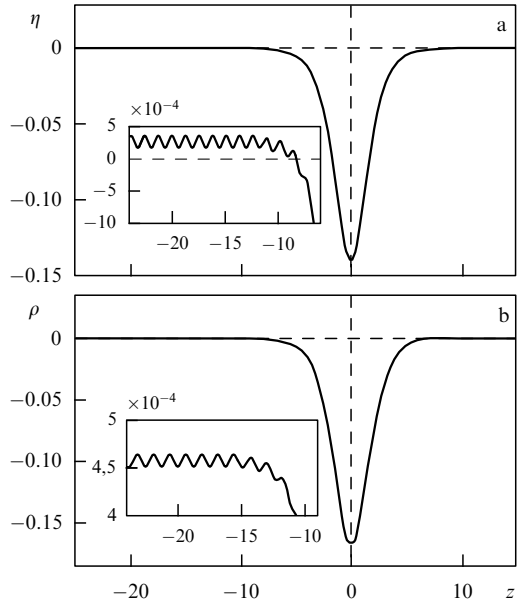

Figure 4. Acoustic compression soliton against the background of a low-amplitude optical phonon ($\gamma = 0.1$, $s = 1.1$): (a) soliton profile for transverse displacements; (b) the same for longitudinal displacements.

Numerical simulation of the time evolution of compression solitons proves their dynamic stability. Solitons travel along the chain at a constant speed without emitting phonons. Upon collision, solitons interact like elastic particles: they bounce without emission of phonons or change of shape (Fig. 5). The interaction of solitons becomes inelastic only near the right-hand bound on a soliton velocity.

2.4 Supersonic extension solitons

As indicated above, geometrical anharmonism at velocities $s > s_1$ precludes the existence of acoustic compression solitons, but may promote the existence of extension solitons. Numerical analysis of the discrete set of equations of motion (3), (4) reveals that there are no stable solutions corresponding to extension solitons. There are, however, certain supersonic values of velocity at which one could anticipate soliton-like extension waves of the zigzag chain. As will be demonstrated, the lifetime of such solitary waves is finite.

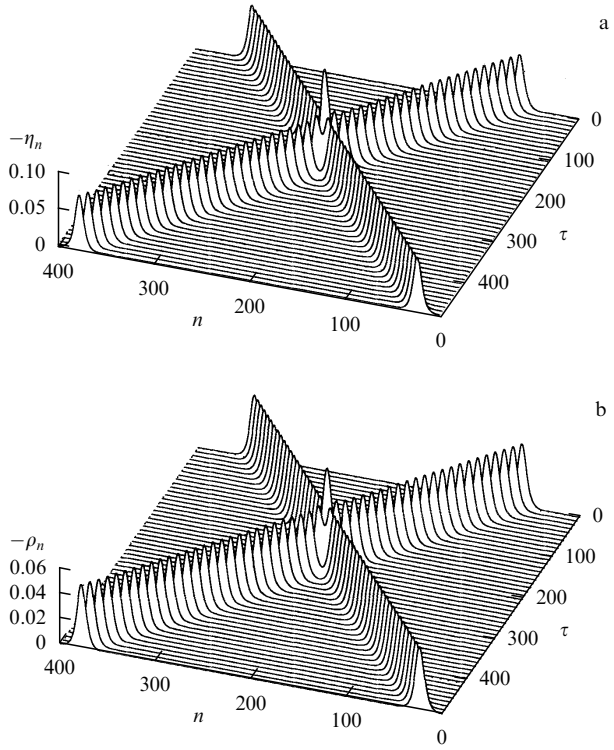

Figure 5. Elastic collision of acoustic compression solitons ($\gamma = 0.1$, $s = 1.05$) in a cyclic chain of $N = 400$ steps: (a) transverse displacements of steps of the chain versus time τ; (b) the same for longitudinal displacements.

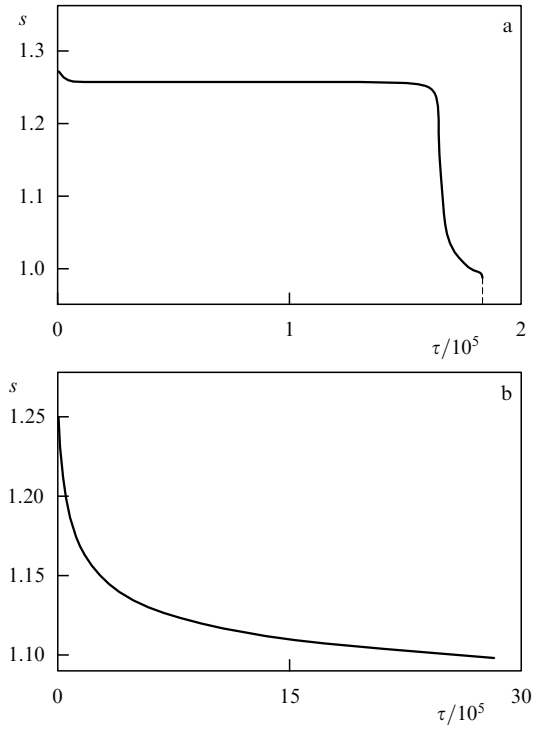

Figure 6. Velocity s of solitary extension wave versus time τ at (a) $\gamma = 1$, and (b) $\gamma = 0.1$.

Indeed, the topology of a zigzag chain admits the existence of solitary extension waves with the asymptotic behaviour

$$v_n \to 0, \quad n \to -\infty; \quad v_n \to h, \quad n \to +\infty; \quad \rho_n \to 0, \quad n \to \pm\infty. \tag{11}$$

Application of the pseudospectral method to the discrete set of equations of motion (3), (4) in the class of smooth functions with asymptotics (11) for arbitrary velocity $s > 1$ gives only an approximate solution. Let us consider a particular value of the velocity and do a numerical simulation of the dynamics of approximate solution in the infinite chain. For this purpose we integrate the set of equations of motion in a finite chain

$$\frac{d^2\rho_n}{d\tau^2} = P_{n+1} - 2P_n + P_{n-1} + Q_{n+2} - Q_{n+1} - Q_n + Q_{n-1}, \tag{12}$$

$$\frac{d^2v_n}{d\tau^2} = -S_{n-1} - S_n + T_{n+1} - T_{n-1}, \tag{13}$$

where $n = 1, 2, \ldots, N$. We set $N = 300$ and introduce viscous friction at the ends of the chain to ensure absorption of phonons emitted by the nonlinear wave (the condition of absorbing ends). Now we consider initial conditions corresponding to a nonlinear solitary wave centred around the point $n = 100$. Each time the wave has passed 100 points, we shift it back so as to simulate motion along an infinite chain. The wave velocity s as a function of time τ is shown in Fig. 6. The motion of the wave is accompanied by emission of phonons that gradually slows the wave down.

At $\gamma = 1$ (Fig. 6a), the least emission corresponds to $s = 1.2568$, when the energy of the wave is $E = 0.06912$. At this velocity, the passage of 100 steps of the chain reduces the velocity of the solitary wave by as little as $8 \times 10^{-5}\%$, and the energy by $1 \times 10^{-3}\%$. Further decrease of velocity leads to increased emission of phonons, and thus to a more substantial deceleration of the wave. The emission of phonons increases dramatically at $s < 1.24$ and leads to the decay of the solitary extension wave. In this way, at the initial velocity of $s = 1.3$, the finite lifetime of the solitary wave is $\tau = 183638$, and the wave covers 143,200 steps of the chain.

As the parameter of anharmonism γ decreases, the lifetime of the solitary extension wave becomes greater. At $\gamma = 0.1$ (Fig. 6b), over the entire time of numerical integration $\tau = 2\,824\,436.3$, the wave has covered 2,000,000 steps of the chain, and its velocity s has fallen from 1.25 to 1.09865. The shape of the wave at the end of this period is shown in Fig. 7. In fact, the wave displays the dynamics of a soliton. The amplitude of emitted phonons with respect to the longitudinal component ρ is 0.04% of the amplitude of the wave, whereas the same with respect to the transverse component v is as small as 0.001%. The energy of the wave is $E = 0.0194894$, and the velocity $s = 1.098632$. The passage of 100 steps of the chain reduces the energy of a solitary wave by $7.7 \times 10^{-5}\%$, and the velocity by as little as $7.3 \times 10^{-5}\%$. Similar dynamic behaviour is shown by a solitary extension wave in the case of small anharmonism ($\gamma = 0.01$), and in the absence of anharmonism ($\gamma = 0$).

Let us consider the interaction of solitary extension waves and compression solitons. For this purpose we do a numerical simulation of their collision in a finite chain of $N = 400$ steps. Numerical integration of the set of equations of motion (12) reveals that the collision is inelastic. The collision between solitary extension waves results in the emission of phonons (Fig. 8), and the collision of a solitary extension wave with compression soliton leads to the decay of the wave.

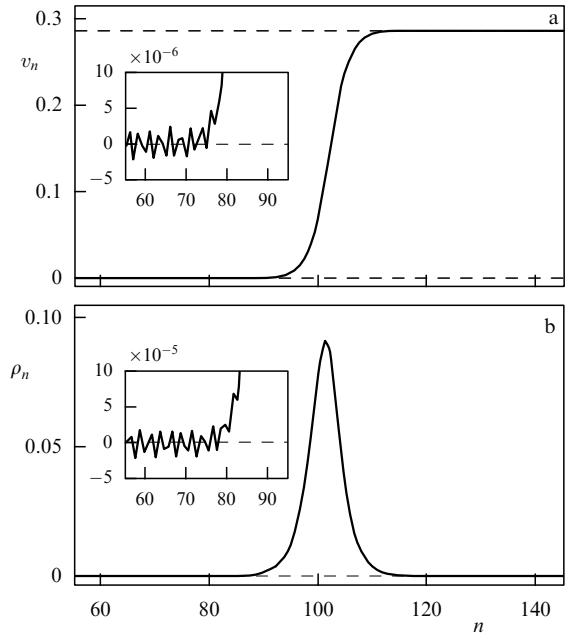

Figure 7. Profile of solitary extension wave with respect to the transverse component v_n (a) and longitudinal component ρ_n (b) in a zigzag chain (n is the site number) with anharmonic constant $\gamma = 0.1$. Wave velocity $s = 1.098632$, energy $E = 0.0194894$.

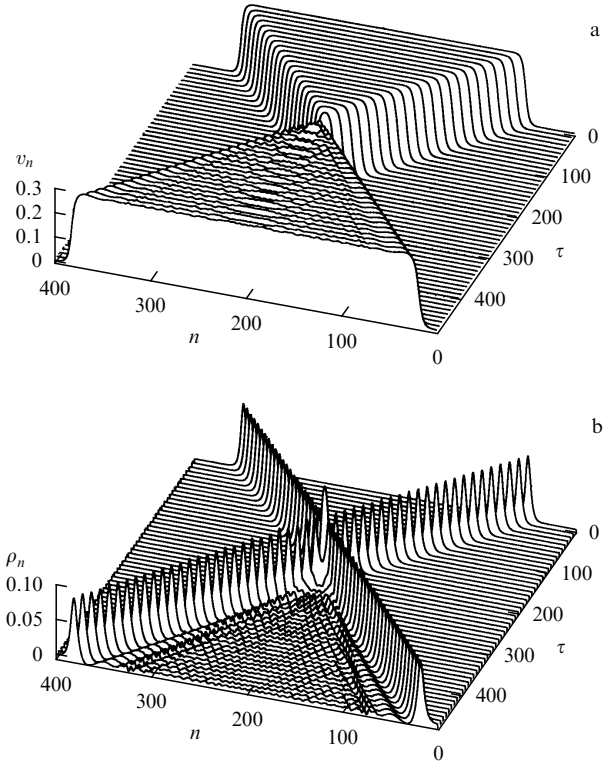

Figure 8. Inelastic collision of solitary extension waves ($\gamma = 0.1$, $s = 1.098632$) in a cyclic chain of $N = 400$ steps: (a) transverse displacements of steps of the chain versus time τ; (b) the same for longitudinal displacements.

The analysis of the simplest two-dimensional model of an alpha-spiral protein molecule indicated that geometrical anharmonism in the zigzag molecular chain delimits the spectrum of velocities of solitons of longitudinal compression of the chain from above. The range of velocities contracts monotonically with the decreasing anharmonism of the interstitial interaction (physical anharmonism). At the same time, geometrical anharmonism gives rise to a new type of nonlinear waves — solitary waves of extension of the zigzag of the chain, which display practically soliton dynamics near a certain selected supersonic velocity value.

3. Extension solitons in a polyethylene molecule

Although the problem of the linear dynamics of the polyethylene molecule was studied by Kirkwood [43] over half a century ago, its nonlinear extension has only recently become the subject of theoretical analysis [36, 37]. The interest was evoked by the recognition of the importance of localized soliton-type nonlinear excitations for the process of mechanical destruction of one-dimensional crystals [44, 45]. It turned out that the transition from the rectilinear chain to the transzigzag conformation leads to a qualitative change in the type of the soliton solutions: instead of compression solitons, the role of nonlinear elementary excitations is now played by extension solitons [36, 37]. The latter owe their existence not to the physical but to the geometrical nonlinearity of the transzigzag, which is not present in the longitudinal dynamics of the rectilinear chain.

This conclusion is reached in the approximation of infinitely rigid valent bonds — that is, only considering the deformation of valence angles. A more advanced study of nonlinear dynamics of the transzigzag conformation was performed in Refs [46, 47], where a model involving deformations of valent bonds and valence angles was used for finding the soliton solutions describing the motion of local extension regions along the transzigzag. These solitons were shown to exhibit a relatively narrow spectrum of supersonic velocities.

3.1 Flat model of a polyethylene macromolecule

In the study of low-energy dynamic processes in the polyethylene molecule, the motion of hydrogen atoms with respect to the backbone is not important, and the approximation of united atoms may be used. Consider a molecule of polyethylene $(CH_2\text{–})_x$ in the transzigzag conformation. At equilibrium, the backbone of the molecule has a flat zigzag structure characterized by a step $\rho_0 = 1.53$ A (the equilibrium length of the valent bond CH_2-CH_2), and a zigzag angle $\theta_0 = 113^\circ$ (the equilibrium valence angle $CH_2-CH_2-CH_2$). The transzigzag structure is shown schematically in Fig. 9a.

Let the transzigzag be directed along the x axis, and lie in the xy plane; then the nth site of the chain at equilibrium will have the coordinates

$$x_n^0 = nl_x\,, \qquad y_n^0 = (-1)^n\,\frac{l_y}{2}\,,$$

where $l_x = \rho_0 \sin(\theta_0/2)$ and $l_y = \rho_0 \cos(\theta_0/2)$ are the longitudinal and the transverse steps of the zigzag of the chain. It is convenient to go over from the absolute coordinates of the nth point x_n, y_n to the relative coordinates

$$u_n = x_n - x_n^0\,, \qquad v_n = (-1)^{n+1}(y_n - y_n^0)\,.$$

Here u_n, v_n define, respectively, the longitudinal and the transverse displacements of the nth point from its equili-

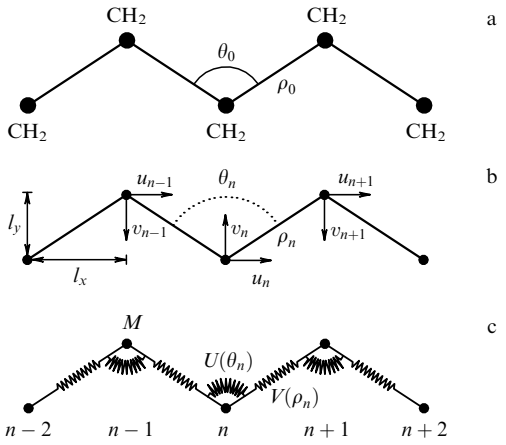

Figure 9. (a) Structure of the polyethylene molecule $(CH_2)_\infty$, (b) selection of local coordinate systems, (c) flat mechanical model of macromolecule.

brium position, the positive direction of the transverse displacement being towards the centre of the zigzag (Fig. 9b). The length of the nth valent bond and the cosine of the nth valence angle are, respectively:

$$\rho_n = \sqrt{(l_x - w_n)^2 + (l_y - z_n)^2}\,,$$

$$\cos(\theta_n) = -\frac{a_{n-1}a_n - b_{n-1}b_n}{\rho_{n-1}\rho_n}\,,$$

where $w_n = u_n - u_{n+1}$ and $z_n = v_n + v_{n+1}$ are the longitudinal and the transverse contractions of the nth unit of the chain; $a_n = l_x - w_n$, $b_n = l_y - z_n$.

The Hamiltonian of the chain may be written as

$$H = \sum_n \left[\frac{1}{2}\,M(\dot{u}_n^2 + \dot{v}_n^2) + V(\rho_n) + U(\theta_n)\right]. \qquad (14)$$

Here the mass of the unit of the chain is $M = 14m_\mathrm{p}$ (m_p is the proton mass),

$$V(\rho_n) = D_0\{1 - \exp[-\beta(\rho_n - \rho_0)]\}^2$$

is the potential of the nth valent bond, and

$$U(\theta_n) = \frac{1}{2}\,\varepsilon(\cos\theta_n - \cos\theta_0)^2$$

is the potential of the nth valence angle. According to Ref. [48], the energy of the valent bond is $D_0 = 334.72$ kJ mol^{-1}, the parameter $\beta = 19.1$ nm^{-1}, and $\varepsilon = 130.122$ kJ mol^{-1}. In Ref. [49], a higher energy value was used, $\varepsilon = 529$ kJ mol^{-1}.

The flat mechanical model of the transzigzag under consideration is shown in Fig. 9c.

3.2 Low-amplitude transzigzag vibrations

The dispersion equation for low-amplitude transzigzag vibrations was first developed by Kirkwood [43]. A detailed proof can be found in Ref. [46], so here we shall skip most of the intermediate calculations.

The set of equations of motion

$$M\ddot{u}_n = -\frac{\partial H}{\partial u_n}\,, \qquad M\ddot{v}_n = -\frac{\partial H}{\partial v_n}\,, \qquad n = 0, \pm1, \pm2, \ldots \qquad (15)$$

corresponds to Hamiltonian (14). We linearize this system and seek its solution in the form of a harmonic wave

$$u_n(t) = A\exp\mathrm{i}[\Omega t + kn]\,,$$

$$v_n(t) = B\exp\mathrm{i}\left[\Omega t + k\left(n + \frac{1}{2}\right)\right],$$

where ω is the circular frequency, and $-\pi \leqslant k \leqslant \pi$ is the dimensionless wave vector. Then the dispersion equation has the form

$$\Omega_\pm^2(k) = \omega_0^2(k) \pm \sqrt{\omega_0^4(k) - \omega_1^4(k)}\,, \qquad (16)$$

where

$$\omega_0^2(k) = C_1(1 + \cos\theta_0\cos k) + 2C_2(1 + \cos k)(1 - \cos\theta_0\cos k)\,,$$

$$\omega_1^4(k) = 8C_1C_2(1 + \cos k)\sin^2 k\,.$$

Here the rigidity parameters are $C_1 = K_1/M$, $C_2 = K_2/M\rho_0^2$, where the rigidity of the valent bond is

$$K_1 = \frac{\mathrm{d}^2}{\mathrm{d}\rho^2}\,V(\rho)\bigg|_{\rho=\rho_0} = 2D_0\beta^2 = 405.53\ \mathrm{N\,m^{-1}}\,,$$

and that of the valence angle

$$K_2 = \frac{\mathrm{d}^2}{\mathrm{d}\theta^2}\,U(\theta)\bigg|_{\theta=\theta_0} = \varepsilon\sin^2\theta_0 = 18.308\times10^{-20}\ \mathrm{J}\,.$$

The shape of the dispersion curve (16) is illustrated in Fig. 10. The upper branch $\Omega = \Omega_+(k)$ corresponds to the high-frequency optical phonons of the transzigzag, and the lower branch $\Omega = \Omega_-(k)$ to the low-frequency optical phonons. The frequency of acoustic phonons tends to zero as $k \to 0$ and $k \to \pi$. These extreme values of the wave number correspond to the long-wave (smooth) longitudinal and bending waves of the zigzag.

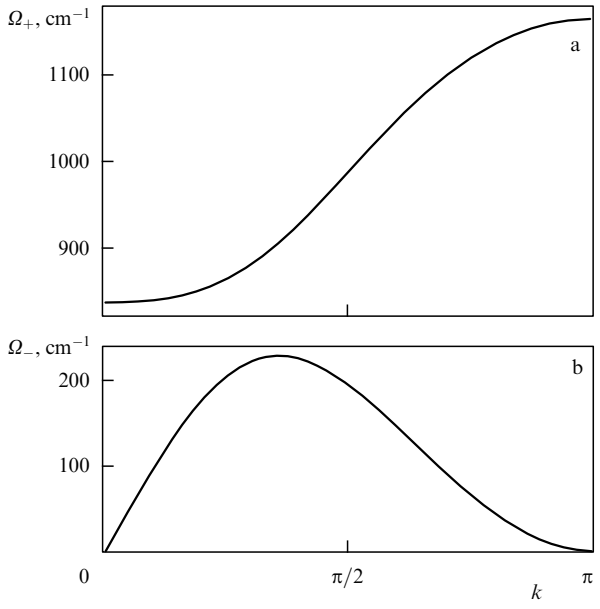

Figure 10. (a) Optical, and (b) acoustic branches of dispersion curve of the transzigzag.

The velocity of the long-wave longitudinal acoustic phonons (the speed of sound) is given by

$$c_0 = l_x \lim_{k\to 0} \frac{\Omega_-(k)}{k} = \frac{2\sqrt{K_2/M}\tan(\theta_0/2)}{\sqrt{1+4\delta\tan(\theta_0/2)}},$$

where the dimensionless parameter

$$\delta = \frac{C_2}{C_1} = \frac{K_2}{K_1\rho_0^2}$$

defines the ratio of the rigidity of the valence angle to that of the valent bond (at $\varepsilon = 130.122$ kJ mol^{-1} we have $\delta = 0.01929$; at $\varepsilon = 529$ kJ mol^{-1} this parameter is $\delta = 0.07841$). As it turns out, the rigidity of the valent bond is two orders of magnitude greater than that of the valence angle. One could well have put up with the approximation of an infinitely rigid valent bond $\delta = 0$ ($K_1 = \infty$), but in this approximation even at $\delta = 0.01929$ the speed of sound

$$\bar{c}_0 = 2\sqrt{\frac{K_2}{M}}\tan\frac{\theta_0}{2} = 8449 \text{ m s}^{-1}$$

differs considerably from the exact value of $c_0 = 7790$ m s$^{-1} = 0.92210\bar{c}_0$. Such a substantial deviation of the speed of sound makes it necessary to take the deformation of valent bonds into account.

3.3 Solitons of longitudinal transzigzag extension

The set of equations of motion (15) is so complicated as to defy analytical treatment (unlike the case of infinitely rigid valent bonds). The use of a pseudospectral method for finding the shape of the soliton is not justified owing to the complexity of the system of equations (15). We shall use a simpler numerical technique of soliton analysis [50], according to which, for every value of the velocity c, the soliton solution $u_n(t) = u(nl_x - ct)$, $v_n(t) = v(nl_x - ct)$, $n = 0, \pm 1, \pm 2, \ldots$ is sought as an extreme point of a certain functional that corresponds in the continuous approximation to the equations of motion of the system. The scheme of application of this technique to the model under consideration is described in Appendix 6.2.

Assume that $\{w_n^0, v_n^0\}_{n=1}^N$ is our soliton solution with the centre of symmetry at the site $n = N/2$. Then the relevant soliton will be characterized by the energy

$$E = \sum_{n=2}^{N-1}\left\{\frac{c^2 M}{24 l_x^2}\left[16w_n^2 - (w_n + w_{n+1})^2 + 16(v_{n+1} - v_n)^2 - (v_{n+2} - v_n)^2\right] + V(\rho_n) + U(\theta_n)\right\},$$

the total contraction of the chain

$$R = \sum_{n=1}^{N} w_n,$$

the root-mean-square width measured in periods of the chain

$$D = 2\sqrt{\sum_{n=1}^{N}\frac{(n-m)^2 w_n}{R}},$$

where the point

$$m = \frac{1}{2} + \sum_{n=1}^{N}\frac{n w_n}{R}$$

defines the location of the centre of the soliton, as well as the maximum value of the valence angle $A_\theta = \max_n \theta_n$, and the maximum length of the valent bond $A_\rho = \max_n \rho_n$.

Numerical analysis indicated that the form of the soliton solution depends on the value of the dimensionless parameter δ that characterizes the ratio between the physical and geometrical anharmonism. The physical anharmonism is due to the potential of the valent bond, whereas the geometrical anharmonism is due to the potential of the valence angle. Geometrical anharmonism prevails at $\delta < 0.0356$, and physical prevails at $\delta > 0.0356$.

With $\delta = 0.01929$, the set of equations of motion (15) admits three types of soliton solutions. The first type corresponds to a solitary wave of longitudinal transzigzag extension (Fig. 11a) with the amplitude $A_v = \max_n v_n < l_y/2$ (the maximum value of the valence angle in the neighbourhood of localization of the soliton is $A_\theta < \pi$) and asymptotic behaviour $w_n, v_n \to 0$ at $n \to \infty$. The second type is a solitary wave of large-amplitude longitudinal transzigzag extension (Fig. 11b) with asymptotic behaviour $w_n, v_n \to 0$ at $n \to -\infty$, and $w_n \to 0$, $v_n \to l_y$ at $n \to +\infty$. This solitary wave describes the sequential unfolding of valence angles from one equilibrium value $\theta_n = \theta_0$ to the other $\theta_n = 2\pi - \theta_0$. As a result, the chain passes from one ground state $\{w_n \equiv 0,\ v_n \equiv 0\}$ to another $\{w_n \equiv 0,\ v_n \equiv l_y\}$. We have already discussed such a soliton in the flat model of an alpha-spiral. The third type corresponds to a transzigzag solitary extension wave (Fig. 11c) with amplitude $l_y/2 < A_v < l_y$ ($\pi < A_\theta < 2\pi - \theta_0$) and asymptotic behaviour $w_n, v_n \to 0$ at $n \to \infty$. This soliton is essentially a bound state of two opposite-sign solitons of the second type.

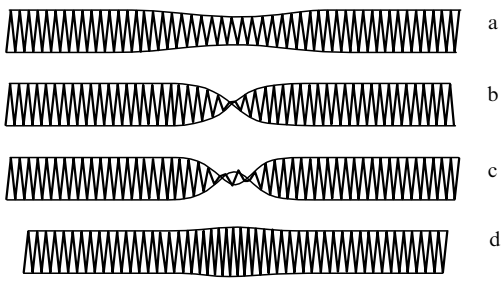

Figure 11. Deformation of the transzigzag corresponding to an extension soliton of the first type, $s = 1.02$ (a), soliton of the second type, $s = 1.05$ (b), soliton of the third type, $s = 1.0738$, $\delta = 0.01929$ (c), and to a compression soliton, $s = 1.035$, $\delta = 0.07841$ (d).

The energy E, the root-mean-square width D, and the overall longitudinal compression of the chain R as functions of the dimensionless soliton velocity $s = c/c_0$ are plotted in Fig. 12. Solitons of the first type display a supersonic spectrum of velocities $1 < s < s_1 = 1.020$. As the velocity of the soliton increases, the energy E and the overall compression of the chain R increase monotonically, and the root-mean-square width D decreases. Solitons of the second type have a supersonic interval of admissible velocities $s_2 = 1.023 < s < s_3 = 1.062$. In this case, E, D, and R all

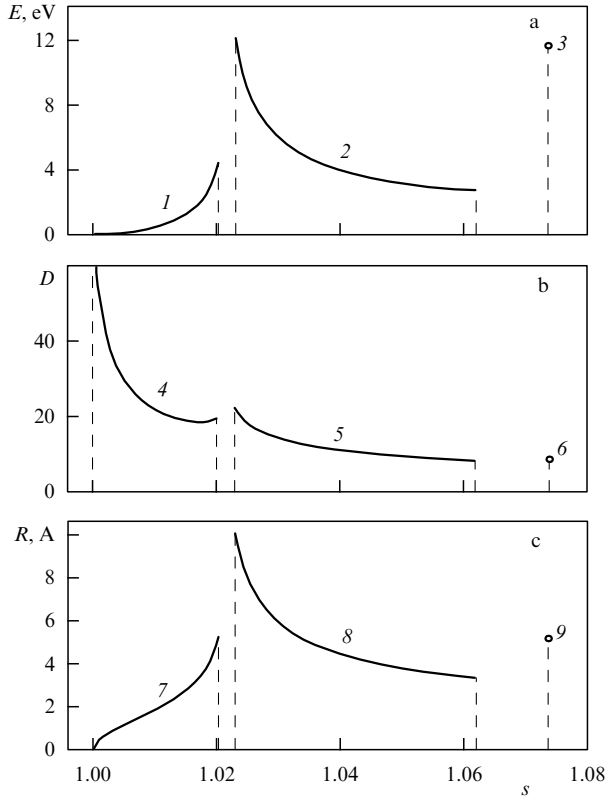

Figure 12. Energy E (a), width D (b), and overall extension of the chain R (c) versus the velocity s of extension soliton of the transzigzag of the first (curves *1*, *4*, *7*), second (curves *2*, *5*, *8*) and third (curves *3*, *6*, *9*) types.

decrease monotonically. Solitons of the third type only exist at one velocity value $s = s_4 = 1.074$.

The characteristic shape of a soliton of the first type is shown in Fig. 13. With respect to its components w_n, v_n, θ_n, the soliton has a characteristic bell-shaped profile of a solitary wave. In the region of localization of a soliton, the molecular

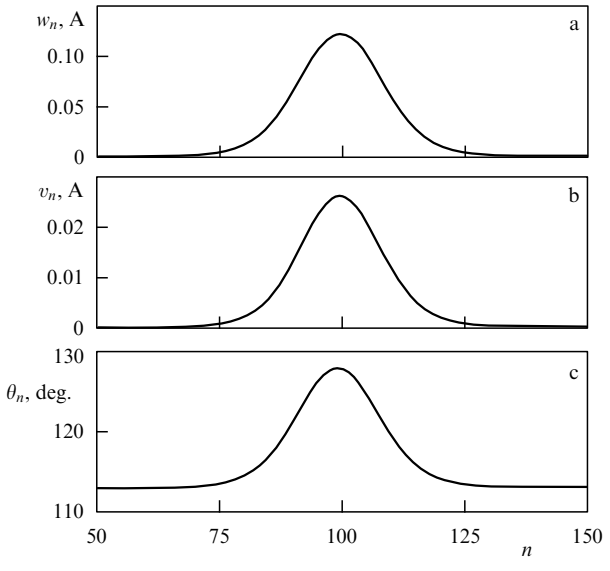

Figure 13. Profile of an extension soliton of the first type with respect to components w_n (a), v_n (b) and θ_n (c) at the initial time $t = 0$ and at the final time $t = 1613.8$ after passing 99999.69 steps of the chain ($s = 1.015$).

chain exhibits longitudinal extension ($w_n > 0$) and transverse compression ($v_n > 0$). The valence angles increase, and the valent bonds stretch out. The existence of such solitons in the zigzag chain is due to the geometrical nonlinearity of the chain rather than to the proper (physical) anharmonism of the intermolecular potentials. This is the fundamental distinction between the transzigzag model and the model of a two-dimensional alpha-spiral.

As the velocity increases, the energy and the amplitude of the soliton increase monotonically, and at $s = s_1$ attain their maximum values of $E_m = 4.6$ eV, $R_m = 5.3$ A. The width of the soliton decreases, but always remains greater than 18 steps of the chain — in other words, the extension soliton always complies with our *a priori* assumption that the profile exhibits a smooth dependence on the number of the step. The particular values of energy E, width D, amplitude R, increments of valence angle $\Delta\theta = A_\theta - \theta_0$ and valent bond $\Delta\rho = A_\rho - \rho_0$ are presented in Table 2. We see that, as the velocity s increases, in the region of localization of the soliton the deformations of angles and bonds increase monotonically but always remain $\Delta\theta < 27^\circ$ for the valence angle, and $\Delta\rho < 0.05$ A for the valent bond.

Table 2. Energy E, width D, overall compression of the chain R, amplitude of extension of valence angle $\Delta\theta$ and amplitude of extension of valent bond $\Delta\rho$ for different values of the velocity s of the soliton of transzigzag extension of the first type.

s	E, eV	D	R, A	$\Delta\theta$, deg.	$\Delta\rho$, A
1.000	0	∞	0	0	0
1.002	0.03	41.9	0.6	1.5	0.002
1.004	0.10	31.2	1.0	3.3	0.005
1.006	0.21	26.7	1.3	5.2	0.008
1.009	0.38	23.4	1.6	7.2	0.012
1.011	0.58	21.3	1.9	9.4	0.016
1.013	0.87	19.9	2.3	12.0	0.021
1.015	1.30	18.9	2.7	15.0	0.026
1.017	1.99	18.4	3.3	18.6	0.034
1.019	3.39	18.8	4.4	24.8	0.044
1.020	4.60	19.6	5.3	26.9	0.051

With the second value of the parameter $\delta = 0.078419$, the set of equations of motion (15) has a soliton solution corresponding to a solitary wave of longitudinal transzigzag compression (see Fig. 11d). In the region of localization of the soliton there occurs contraction of the valence angles and bonds. The soliton has a finite velocity range $1 < s \leqslant 1.035$.

The velocity range of an acoustic soliton versus the dimensionless parameter δ is shown in Fig. 14. At $\delta < \delta_0 = 0.0356$, the soliton is a solitary extension wave, and at $\delta > \delta_0$ a solitary transzigzag compression wave. In a chain with $\delta = 0$ (approximation of infinitely rigid valent bond), the velocity range of the soliton is $1 < s < s_1 = 1.095$. As δ increases, the upper limit of the velocities s_1 decreases steadily. At the threshold value $\delta = \delta_0$, the geometrical and physical anharmonisms cancel out, and the velocity range vanishes ($s_1 = 1$). A further increase of δ leads to monotone growth of the velocity range.

Numerical simulation of the dynamics indicated that the soliton of the first type is dynamically stable at all values of the velocity $1 < s < s_1$. It moves at a constant speed, and completely retains its original shape. For example, with the initial dimensionless velocity $s = 1.015$ ($c = 7906.85$ m s^{-1}, $\delta = 0.01929$), the soliton passed 99999.694 steps of the chain for 1613.8 ps, and had a final velocity of $s = 1.014995$ ($c = 7906.81$ m s^{-1}). As shown in Fig. 13, the final shape of

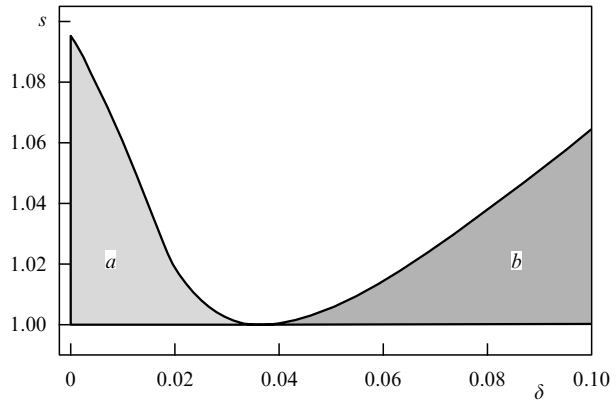

Figure 14. (*a*) Region of existence of an acoustic soliton of extension, and (*b*) the region of existence of a soliton of transzigzag compression in the space of dimensionless parameters δ and s.

the soliton is exactly the same as in the beginning. Solitons interact as elastic particles. Their collisions result in elastic reflection without emission of phonons or change of shape (Fig. 15). It is only near the limiting velocity s_1 that the interaction of solitons becomes inelastic: collision is accompanied with emission of phonons. Thus, near the speed of sound the extension solitons of the first type display definite particle-like properties. Solitons of the second type are unstable. When moving they emit phonons and soon perish. Solitons of the third type are stable at the velocity $s = s_4$. They move along the chain at a constant speed and retain their shape. Interaction between solitons of the third type is not elastic; collisions between solitons lead to their destruction.

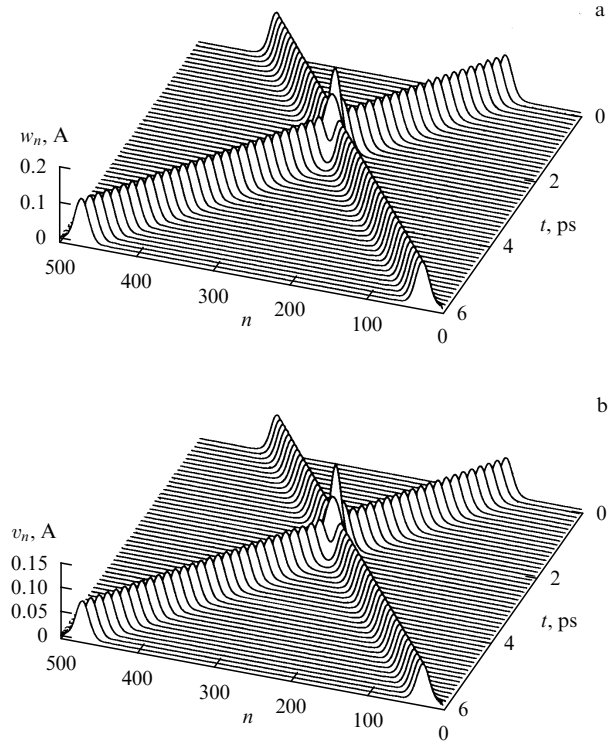

Figure 15. Elastic collision of extension solitons of the first type in a cyclic chain of $N = 500$ steps: (a) longitudinal displacements of steps of the chain versus time t; (b) the same for transverse displacements.

The above analysis of the transzigzag model indicated that an isolated flat macromolecule of polyethylene may host dynamically stable extension solitons that display a relatively narrow spectrum of supersonic velocities. The existence of solitons is due to the geometrical anharmonism of the zigzag chain rather than to the physical anharmonism of potentials of interstitial interaction.

4. Nonlinear dynamics of a flat zigzag chain of hydrogen bonds

The shape of a flat zigzag is displayed by the chains of hydrogen bonds ...H–X...H–X...H–X... in molecules of hydrogen halides HX (X = F, Cl, Br, I) [38–40]. The zigzag shape of the chain is due to the orientational interaction between adjacent molecules. A similar shape is also displayed by the chains of hydrogen bonds ...O–H...O–H...O–H..., formed in the protein macromolecules by the amino acid groups ROH containing the hydroxyl OH^- radical (serine, threonine, tyrosine). Such chains convey protons in the protein proton channels [51–53], which makes the study of their nonlinear dynamics especially interesting.

The particular values of the parameters of chains of hydrogen bonds $(HX...)_x$ (X = O, F, Cl, Br, I) are given in Table 3. Here, r_0 is the length of the valent bond H–X, a and α are the step and angle of the zigzag of the chain [40], μ and Q are the dipole and the quadrupole moments of isolated HX molecule [54], and $I = m_p r_0^2$ is the moment of inertia of the molecule (m_p is the proton mass). As follows from the table, the chain of hydrogen-bonded hydrogen fluoride molecules is closest in parameters to the chain of hydrogen-bonded hydroxyl groups. For this reason we shall consider this chain as the model system for the zigzag chain of hydrogen bonds.

Table 3. Values of parameters of zigzag chains of hydrogen bonds HX...HX...HX.

HX	r_0, A	a, A	α, deg.	μ, 10^{-18} CGS cm	Q, 10^{-26} CGS cm^2	I, 10^{-40} g cm^2
HO	1.01	2.76	120	1.58	—	1.706
HF	0.97	2.50	117	1.736	2.6	1.574
HCl	1.275	3.688	93.5	1.07	3.8	2.719
HBr	1.414	3.927	91.8	0.783	4.0	3.344
HI	1.604	4.23	90	0.382	6.0	4.303

4.1 Model potential of a hydrogen bond

The interaction between diatomic polar HF molecules is usually described by the 12–6–1 potential [55]

$$U = \sum_{i_1=1}^{3}\sum_{i_2=1}^{3}\frac{q_{i_1}q_{i_2}}{r_{i_1 i_2}} + 4\epsilon\left[\left(\frac{\sigma}{r}\right)^{12} - \left(\frac{\sigma}{r}\right)^{6}\right] \qquad (17)$$

with seven adjusting parameters: two Lennard–Jones parameters ϵ and σ; three charges q_1, q_2, and q_3 ($q_1 + q_2 + q_3 = 0$) in line with the valent bond, and three distances r_1, r_2, and r_3 from each charge to the centre of fluorine atom. In Eqn (17), $r_{i_1 i_2}$ is the distance between the charge q_{i_1} of the first HF molecule and the charge q_{i_2} of the second molecule.

The values of parameters in the interaction potential (17) can be chosen using the results of quantum mechanical calculation of the potential energy surface of the dimer

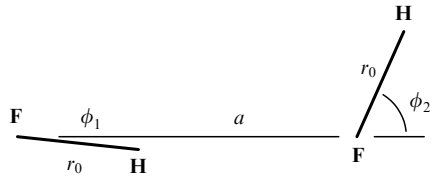

Figure 16. Equilibrium configuration of an HF...HF dimer.

HF...HF [56]. Figure 16 shows the most energy-advantageous dimer configuration determined by two angles $\phi_1 = -6.5^\circ$, $\phi_2 = 67.7^\circ$, and one length $a = 2.76$ A. The bond energy is $E_1 = 0.191$ eV. The dimer may occur in either of two equivalent ground states $\{\phi_1, \phi_2, a\}$ and $\{\pi - \phi_2, \pi - \phi_1, a\}$. In addition, there is an intermediate symmetric metastable state $\{-\phi_3, \pi - \phi_3, b\}$ with the energy $E_2 = E_1 + E_0$, where $E_0 = 0.068$ eV is the height of the energy barrier of dimer interconversion.

The exact values of the dipole μ and quadrupole Q moments of the HF molecule, and the dimer parameters ϕ_1, ϕ_2, a, E_1, and E_0 define unambiguously all seven parameters of the potential of intermolecular interaction (17):

$$q_1 = -1.252\,\mathrm{e}, \quad q_2 = 0.485\,\mathrm{e}, \quad q_3 = 0.767\,\mathrm{e},$$
$$r_1 = -0.35\,\mathrm{A}, \quad r_2 = 0.861\,\mathrm{A}, \quad r_3 = -0.644\,\mathrm{A},$$
$$\epsilon = 0.0192\,\mathrm{eV}, \quad \sigma = 2.855\,\mathrm{A},$$

where e is the electron charge.

4.2 Low-amplitude vibrations of the chain of hydrogen bonds

Consider an isolated chain of hydrogen bonds ...H–F... H–F...H–F... with step $a = 2.76$ A and zigzag angle $\alpha = \pi - \phi_2 - \phi_1 = 118.8^\circ$ (Fig. 17). At equilibrium, all the HF molecules deviate from the direction of the zigzag by the angle $-\phi_1$.

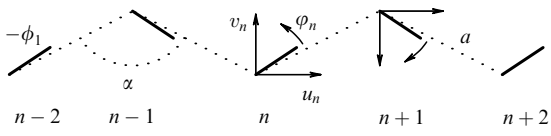

Figure 17. Selection of the system of local coordinates for the chain of hydrogen bonds HF...HF...HF.

Assume that the zigzag of the chain is directed along the x axis and lies in the xy plane; then the location of the nth molecule of the chain at equilibrium position is fixed by the coordinates of the fluorine atom $x_n^\circ = nl_x$, $y_n^\circ = (-1)^n l_y/2$, where $l_x = a\sin(\alpha/2)$ and $l_y = a\cos(\alpha/2)$ are the longitudinal and the transverse steps of the zigzag of the chain, and the angle $\psi_n^\circ = (-1)^{n+1}\psi^0$, $\psi^0 = (\pi - \alpha)/2 - \phi_1$ defines the orientation of the molecule. As before, it will be convenient to go over from absolute coordinates x_n, y_n, ψ_n to the relative coordinates

$$u_n = x_n - x_n^\circ, \quad v_n = (-1)^{n+1}(y_n - y_n^\circ),$$
$$\varphi_n = (-1)^{n+1}(\psi_n - \psi_n^\circ).$$

Here u_n, v_n, φ_n define, respectively, the longitudinal and transverse displacements and the rotation of the nth molecule from its equilibrium position (the positive direction for transverse displacement and rotation is the direction towards the centre of the zigzag, see Fig. 17).

The Hamiltonian of the chain may be expressed as

$$H = \sum_n \left[\frac{1}{2}M(\dot{u}_n^2 + \dot{v}_n^2) + \frac{1}{2}I\dot{\varphi}_n^2 + V(u_{n+1} - u_n, v_n + v_{n+1}, \varphi_n, \varphi_{n+1}) \right], \qquad (18)$$

where $M = 19m_\mathrm{p}$ is the mass of the molecule, and $I = 1.706 \times 10^{-14}$ g cm^2 is the moment of inertia. The potential of the intermolecular interaction is

$$V(u, v, \varphi, \psi) = U(0, 0, \psi^0 + \varphi;\, l_x + u, l_y - v, -\psi^0 - \psi).$$

The Hamiltonian of the chain (18) enters the set of equations of motion

$$\begin{aligned}
M\ddot{u}_n &= V_u(u_{n+1} - u_n, v_{n+1} + v_n, \varphi_n, \varphi_{n+1}) \\
&\quad - V_u(u_n - u_{n-1}, v_n + v_{n-1}, \varphi_{n-1}, \varphi_n), \\
-M\ddot{v}_n &= V_v(u_{n+1} - u_n, v_{n+1} + v_n, \varphi_n, \varphi_{n+1}) \\
&\quad + V_v(u_n - u_{n-1}, v_n + v_{n-1}, \varphi_{n-1}, \varphi_n), \\
-I\ddot{\varphi}_n &= V_\varphi(u_{n+1} - u_n, v_{n+1} + v_n, \varphi_n, \varphi_{n+1}) \\
&\quad + V_\psi(u_n - u_{n-1}, v_n + v_{n-1}, \varphi_{n-1}, \varphi_n), \qquad (19)
\end{aligned}$$

where $n = 0, \pm 1, \pm 2, \ldots$

For small-amplitude displacements, the set of equations (19) in the linear approximation takes the form

$$\begin{aligned}
M\ddot{u}_n &= V_{uu}(u_{n+1} - 2u_n + u_{n-1}) + V_{uv}(v_{n+1} - v_{n-1}) \\
&\quad + V_{u\varphi}(\varphi_n - \varphi_{n-1}) + V_{u\psi}(\varphi_{n+1} - \varphi_n), \\
-M\ddot{v}_n &= V_{uv}(u_{n+1} - u_{n-1}) + V_{vv}(v_{n-1} + 2v_n + v_{n+1}) \\
&\quad + V_{v\varphi}(\varphi_n + \varphi_{n-1}) + V_{v\psi}(\varphi_{n+1} + \varphi_n), \\
-I\ddot{\varphi}_n &= V_{u\varphi}(u_{n+1} - u_n) + V_{u\psi}(u_n - u_{n-1}) \\
&\quad + V_{v\varphi}(v_n + v_{n+1}) + V_{v\psi}(v_n + v_{n-1}) \\
&\quad + (V_{\varphi\varphi} + V_{\psi\psi})\varphi_n + V_{\varphi\psi}(\varphi_{n+1} + \varphi_{n-1}), \qquad (20)
\end{aligned}$$

where all the second partial derivatives $V_{uu}, V_{uv}, \ldots, V_{\psi\psi}$ are taken at the point $u = 0$, $v = 0$, $\varphi = 0$, $\psi = 0$. We seek a solution of the linear set of equations (20) in the form of a harmonic wave

$$\begin{aligned}
u_n(t) &= A_1 \exp\left[\mathrm{i}(\Omega t + kn)\right], \\
v_n(t) &= A_2 \exp\left[\mathrm{i}(\Omega t + kn)\right], \\
\varphi_n(t) &= A_3 \exp\left[\mathrm{i}(\Omega t + kn)\right], \qquad (21)
\end{aligned}$$

where Ω is the circular frequency, $-\pi \leqslant k \leqslant \pi$ is the dimensionless wave vector. After substitution of expressions (21) into the set of linear equations (20) and some straightforward algebra we get the dispersion equation of sixth power in Ω. Skipping the intermediate calculations, we shall go straight to the shape of the dispersion curve.

The dispersion curve for low-amplitude oscillations consists of three branches as shown in Fig. 18. The upper branch 263 cm$^{-1} \leqslant \Omega_\mathrm{or}(k) \leqslant 487$ cm^{-1} corresponds to high-

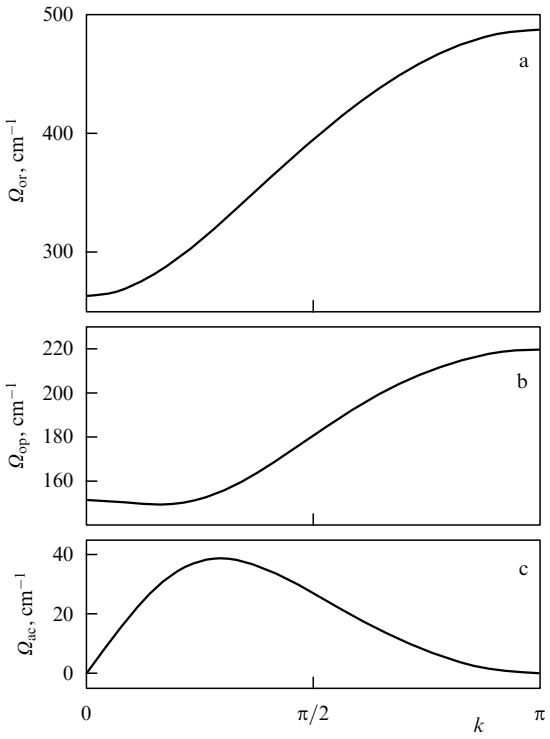

Figure 18. Orientation (a), optical (b) and acoustic (c) branches of the dispersion curve of the zigzag chain of hydrogen bonds HF...HF...HF.

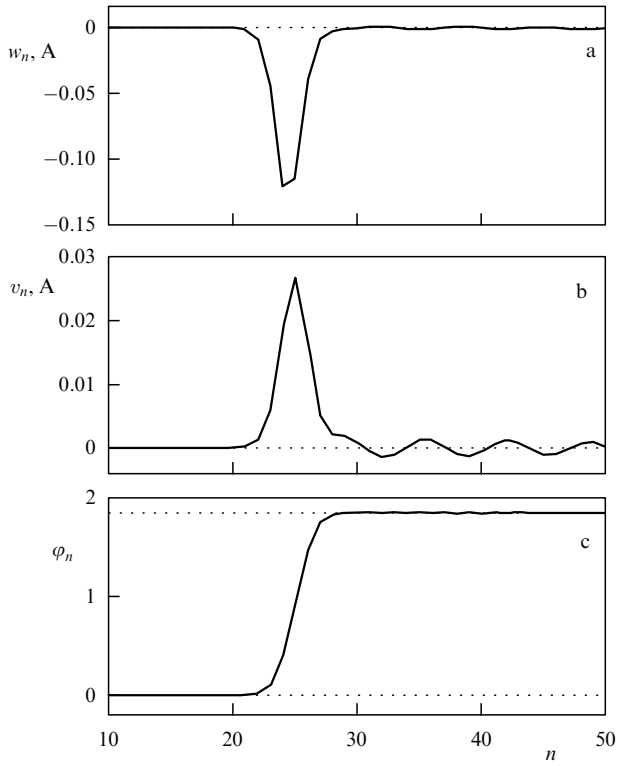

Figure 19. Emission of optical phonons by a positive orientation defect moving from right to left with the dimensionless velocity $s = 2.4$: (a) profile of longitudinal compression of the chain $w_n = u_{n+1} - u_n$; (b) transverse displacements v_n, and (c) angles of rotation of molecules φ_n.

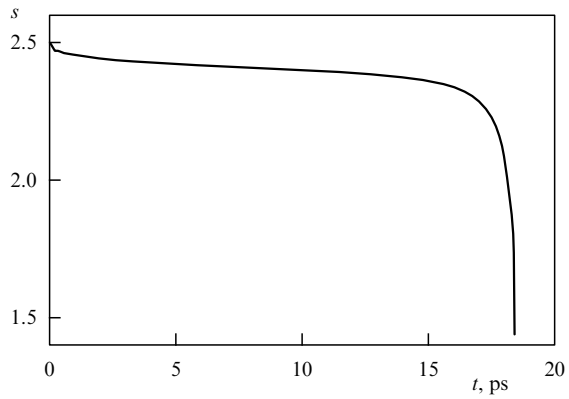

Figure 20. Dimensionless velocity s of the positive orientation defect versus time t.

frequency orientation oscillations of the molecules, the middle branch 149 cm$^{-1} \leqslant \Omega_{op}(k) \leqslant 219$ cm^{-1} corresponds to optical phonons of the zigzag, and the lower branch $0 \leqslant \Omega_{ac}(k) \leqslant 38$ cm^{-1} to low-frequency acoustic phonons. The two lower branches behave in the same way as the acoustic and optical branches of the two models of zigzag chains discussed above. The speed of the long-wave longitudinal acoustic phonons is

$$c_0 = l_x \lim_{k\to 0} \frac{\Omega_{ac}(k)}{k} = 3046.2822 \text{ m s}^{-1}.$$

4.3 Nonlinear dynamics of the chain of hydrogen bonds

Numerical analysis of the nonlinear system of dynamic equations (19) revealed that, in spite of the pronounced anharmonism of the potential of interstitial interaction, the system under consideration does not host any solitons of compression or extension. Soliton-like dynamics is only featured by the positive orientation defect corresponding to the consecutive transition of the chain from one ground state $\{u_n \equiv 0, v_n \equiv 0, \varphi_n \equiv 0\}$ to another equivalent state $\{u_n \equiv 0, v_n \equiv 0, \varphi_n \equiv \alpha + 2\phi_1\}$. The passage of the defect is accompanied by the emission of optical phonons (Fig. 19) that leads to its deceleration and eventual destruction. The dimensionless velocity of the defect $s = c/c_0$ versus time is plotted in Fig. 20. The defect travels at supersonic speed. Emission of phonons is minimal at $s = 2.4$, and increases abruptly at $s = 2.3$. Over its lifetime of $t = 18.4$ ps, the defect covered 560 steps of the chain.

The absence of solitons of compression and extension is due to the fact that the physical anharmonism in the case of soft hydrogen bonds is balanced out by the geometrical anharmonism of the chain. If the chain had been linear, the anharmonism of the hydrogen bond would have given rise to supersonic compression solitons: the chain would have featured stable solitary compression waves. However, in a zigzag chain with zigzag angle $\alpha \leqslant 120^\circ$ there are no stable solitary waves of longitudinal compression or extension. Any initial localized excitation will soon smear out. In this way, the geometry of the chain is of fundamental importance for the nonlinear dynamic behaviour of the chain.

5. Conclusions

In this paper we have analyzed the nonlinear dynamics of zigzag molecular chains. The transition from a one-dimensional model of a rectilinear chain to a more realistic flat model of the zigzag chain is found to bring about a fundamental change in the nonlinear dynamics of the chain. The nonlinear effects are no longer due only to the

anharmonism of the interstitial interaction (physical anharmonism). A new important factor comes into play: geometrical anharmonism of opposite sign caused by the zigzag geometry of the chain. Now the possible existence of solitons (solitary longitudinal waves of compression or extension of the chain) depends on the balance between physical and geometrical anharmonisms. We have considered three characteristic types of the zigzag chains:

1. A two-dimensional model of an alpha-spiral protein molecule. The major contribution to nonlinear dynamics here comes from the anharmonism of the hydrogen bonds (physical anharmonism). As a result, compression solitons with a narrow spectrum of supersonic velocities are feasible.

2. A model of a flat polyethylene transzigzag dominated by geometrical anharmonism due to the zigzag-shaped conformation. This model only admits extension solitons, also with a narrow spectrum of supersonic velocities.

3. Finally, we have considered a zigzag chain of hydrogen bonds ...HF...HF...HF..., in which geometrical anharmonism is balanced out by physical anharmonism. As a result, the chain with pronounced anharmonism of interstitial interaction does not admit acoustic solitons, and any initially localized deformation of the chain will smear out.

On the one hand, the two-dimensional nature of molecular chain imposes considerable limitations on the dynamics of solitons (they may only have finite and relatively narrow ranges of admissible velocities). On the other hand, it opens the possibility of simultaneous existence of several types of acoustic solitons. For example, solitons of extension and compression may coexist in the chain.

Our study indicates that one-dimensional models of molecular chains that are still used extensively may lead to wrong conclusions. The geometry of the chain must be taken into account to pursue the possibility of describing physical phenomena in terms of solitary waves.

Two of the authors (A V Savin and L I Manevich) thank the Russian Foundation for Basic Research for financial support (Grants RFBR-97-02-17825, RFBR-98-03-333-66a).

6. Appendices

6.1 Pseudospectral method for finding the shape of a soliton

The pseudospectral method for numerical calculation of the form of a soliton solution was first proposed by Eilbeck and Flesch [41] for the one-dimensional model of an anharmonic chain. Application of this technique to the two-dimensional model of the zigzag chain requires only some minor modifications.

Consider the solution of the discrete system (3), (4) in the form of a solitary wave (9). Then from the system of equations of motion (3), (4) follows the set of equations

$$\begin{aligned} v^2\rho_{zz} = {} & P\left(\rho\left(z+\frac{1}{2}\right),\eta\left(z+\frac{1}{2}\right)\right) - 2P\big(\rho(z),\eta(z)\big) \\ & + P\left(\rho\left(z-\frac{1}{2}\right),\eta\left(z-\frac{1}{2}\right)\right) + Q\big(\rho(z+1),\eta(z+1)\big) \\ & - Q\left(\rho\left(z+\frac{1}{2}\right),\eta\left(z+\frac{1}{2}\right)\right) - Q\big(\rho(z),\eta(z)\big) \\ & + Q\left(\rho\left(z-\frac{1}{2}\right),\eta\left(z-\frac{1}{2}\right)\right), \end{aligned} \tag{A.1}$$

$$\begin{aligned} v^2\eta_{zz} = {} & -S\left(\rho\left(z+\frac{1}{2}\right),\eta\left(z+\frac{1}{2}\right)\right) - 2S\big(\rho(z),\eta(z)\big) \\ & - S\left(\rho\left(z-\frac{1}{2}\right),\eta\left(z-\frac{1}{2}\right)\right) + T\left(\rho\left(z+\frac{1}{2}\right),\eta\left(z+\frac{1}{2}\right)\right) \\ & - T\left(\rho\left(z-\frac{1}{2}\right),\eta\left(z-\frac{1}{2}\right)\right) + T\big(\rho(z+1),\eta(z+1)\big) \\ & - T\big(\rho(z),\eta(z)\big), \end{aligned} \tag{A.2}$$

where $z = n/2 - v\tau$ is the wave variable. The main idea of the method consists in approximating the exact soliton solution $\rho(z)$, $\eta(z)$ with finite Fourier expansions over the interval $-L/2 \leqslant z \leqslant L/2$:

$$\rho(z) \simeq \tilde{\rho}(z) = \sum_{k=0}^{K} a_k e_k(z), \tag{A.3}$$

$$\eta(z) \simeq \tilde{\eta}(z) = \sum_{k=0}^{K} b_k e_k(z), \tag{A.4}$$

where $e_k(z) = \cos(2\pi k/L)$, $k = 0, 1, 2, \ldots, K$. Substitution of expressions (A.3), (A.4) into Eqns (A.1), (A.2) yields the system of two continual equations

$$\begin{aligned} F_1(z) = {} & v^2 \sum_{k=0}^{K} a_k \left(\frac{2\pi k}{L}\right)^2 e_k(z) + \tilde{P}\left(z+\frac{1}{2}\right) \\ & - 2\tilde{P}(z) + \tilde{P}\left(z-\frac{1}{2}\right) + \tilde{Q}(z+1) \\ & - \tilde{Q}\left(z+\frac{1}{2}\right) - \tilde{Q}(z) + \tilde{Q}\left(z-\frac{1}{2}\right), \end{aligned} \tag{A.5}$$

$$\begin{aligned} F_2(z) = {} & v^2 \sum_{k=0}^{K} b_k \left(\frac{2\pi k}{L}\right)^2 e_k(z) - \tilde{S}\left(z+\frac{1}{2}\right) \\ & - 2\tilde{S}(z) - \tilde{S}\left(z-\frac{1}{2}\right) + \tilde{T}\left(z+\frac{1}{2}\right) \\ & - \tilde{T}\left(z-\frac{1}{2}\right) + \tilde{T}(z+1) - \tilde{T}(z), \end{aligned} \tag{A.6}$$

where

$$\begin{aligned} \tilde{P}(z) &= P\left(\sum_{k=0}^{K} a_k e_k(z), \sum_{k=0}^{K} b_k e_k(z)\right), \\ \tilde{Q}(z) &= Q\left(\sum_{k=0}^{K} a_k e_k(z), \sum_{k=0}^{K} b_k e_k(z)\right), \\ \tilde{S}(z) &= S\left(\sum_{k=0}^{K} a_k e_k(z), \sum_{k=0}^{K} b_k e_k(z)\right), \\ \tilde{T}(z) &= T\left(\sum_{k=0}^{K} a_k e_k(z), \sum_{k=0}^{K} b_k e_k(z)\right). \end{aligned}$$

The Fourier coefficients $\{a_k, b_k\}_{k=0}^{K}$ can be found numerically as the roots of the system of $2K$ nonlinear equations

$$\begin{aligned} & F_1(z_i) = 0, \\ & F_2(z_i) = 0, \quad i = 0, 1, \ldots, K-1, \\ & \tilde{\rho}\left(\frac{L}{2}\right) = \sum_{k=0}^{K} a_k e_k\left(\frac{L}{2}\right) = 0, \\ & \tilde{\eta}\left(\frac{L}{2}\right) = \sum_{k=0}^{K} b_k e_k\left(\frac{L}{2}\right) = 0, \end{aligned} \tag{A.7}$$

where $z_i = iL/(2K)$, and the functions $F_1(z)$, $F_2(z)$ are given by Eqns (A.5), (A.6).

This method is capable of giving an unambiguous answer concerning the existence of a soliton at each value of the velocity v. If the system (A.7) admits no soliton solution, this means that there is no soliton motion at this value of the velocity. For numerical solution of the system (A.7) it is sufficient to set $K = 100$, and $L = 10D$, where D is the root-mean-square width of the soliton (11).

6.2 Method of minimization for finding the soliton solution

We seek a solution of the system of equations of motion (15) in the form of a travelling smooth wave of constant profile. For this purpose we set $u_n(t) = u(\xi)$, $v_n(t) = v(\xi)$, where $\xi = nl_x - ct$ is the wave variable, c is the velocity of the wave, and u and v are smooth functions of ξ. Then the Lagrangian corresponding to the system of equations of motion (15)

$$L = \sum_n \left[\frac{1}{2} M(\dot{u}_n^2 + \dot{v}_n^2) - V(\rho_n) - U(\theta_n) \right] \tag{A.8}$$

may be written in the form

$$\bar{L} = \sum_n \left\{ \frac{c^2 M}{24 l_x^2} \left[16 w_n^2 - (w_n + w_{n+1})^2 + 16(v_{n+1} - v_n)^2 - (v_{n+2} - v_n)^2 \right] - V(\rho_n) - U(\theta_n) \right\}. \tag{A.9}$$

The supersonic soliton state of the chain always corresponds to the saddle point of the Lagrangian, and it can therefore be sought as the minimum point of the functional

$$F = \frac{1}{2} \sum_n (\bar{L}_{w_n}^2 + \bar{L}_{v_n}^2) .$$

Thus, for finding the soliton solution (solitary wave) $\{w_n, v_n\}_{n=1}^N$, one must find the conditional minimum

$$F = \frac{1}{2} \sum_{n=2}^{N-1} (\bar{L}_{w_n}^2 + \bar{L}_{v_n}^2) \to \min : w_1 = w_N = v_1 = 0 , \quad v_N = 0(h) . \tag{A.10}$$

The solution of this problem allows all soliton solutions of the nonlinear system (15) to be found numerically — that is, smooth solitary waves of constant profile. The absence of such solutions at some value of the velocity c means that there is no soliton motion at this velocity.

Problem (A.10) was solved numerically by the method of conjugate gradients. The solution was sought on a chain of $N = 400$ steps. The initial point of descent was taken in the form of two symmetrical bell-shaped (or kink) profiles $w(n)$, $v(n)$, centred at the middle of the chain.

The key idea of the method consists in replacing the continuous time derivatives in the Lagrangian (A.8) with their discrete approximations [the transition from the Lagrangian (A.8) to the discrete functional (A.9)]. Therefore, this method is only good for finding 'broad' soliton solutions, whose shape exhibits a smooth dependence on the number n of the site of the chain (the length of chain N must be ten times the width of the soliton solution). Practically, this method is much simpler than the more general pseudospectral method. Because of this, this technique is preferably used for soliton analysis of molecular systems of complex structure, even though it is not capable of finding 'narrow' soliton solutions.

References

1. Bishop A, in *Solitons in Action* (Eds K Lonngren, A Scott) (New York: Academic Press, 1978) [Translated into Russian (Moscow: Mir, 1981) p. 72]
2. Collins M A *Chem. Phys. Lett.* **77** 342 (1981)
3. Collins M A *Adv. Chem. Phys.* **53** 225 (1983)
4. Kosevich A M *Teoriya Kristallicheskoĭ Reshetki: Fizicheskaya Mekhanika Kristallov* (Theory of Crystal Lattice. Physical Mechanics of Crystals) (Khar'kov: Vishcha Shkola, 1988)
5. Davydov A S *Solitony v Molekulyarnykh Sistemakh* (Solitons in Molecular Systems) (Kiev: Naukova Dumka, 1984) [Translated into English (Dordrecht: Kluwer Academic Publ., 1991)]
6. Ginzburg V V, Manevich L I *Vysokomol. Soedin. A* **34** 91 (1992)
7. Ginzburg V V, Manevich L I *Vysokomol. Soedin. A* **34** 98 (1992)
8. Balabaev N N, Manevich L I, Musienko A I, in *Trudy Mezhdunarodnoĭ Konferentsii 'Matematika, Komp'yutery, Obrazovanie'* (Proc. Int. Conf. 'Mathematics, Computers, Education') (Dubna: Izd. OIYaI, 1998) p. 18
9. Manevitch L I, Ryvkina N G, in *Mechanical Modelling of New Electromagnetic Materials* (Ed. R K T Hsieh) (Amsterdam: Elsevier, 1990) p. 155
10. Savin A V, Manevitch L I *Vysokomol. Soedin. A* **40** (6) 931 (1998)
11. Manevitch L I, Smirnov V V *Phys. Lett. A* **165** 365 (1992)
12. Manevich L I et al. *Usp. Fiz. Nauk* **164** 937 (1994) [*Phys. Usp.* **37** 859 (1994)]
13. Manevich L I, Savin A V *Zh. Eksp. Teor. Fiz.* **107** 1269 (1995) [*JETP* **80** 706 (1995)]
14. Manevitch L I, Smirnov V V *J. Phys. C* **7** 255 (1995)
15. Fermi E, Pasta J, Ulam S, in *Collected Works of Enrico Fermi* Vol. 2 (Chicago: University of Chicago Press, 1965) p. 978
16. Zabusky N J, Kruskal M D *Phys. Rev. Lett.* **15** 241 (1965)
17. Zabusky N J *Comput. Phys. Commun.* **5** 1 (1973)
18. Toda M *Phys. Rep.* **18** 1 (1975)
19. Olsen O H, Lomdhal P S, Kerr W C *Phys. Lett. A* **136** 402 (1989)
20. Christiansen P L, Lomdhal P S, Muto V *Nonlinearity* **4** 477 (1990)
21. Muto V, Lomdhal P S, Christiansen P L *Phys. Rev. A* **42** 7452 (1990)
22. Lomdhal P S, Olsen O H, Samuelsen M R *Phys. Lett. A* **152** 343 (1991)
23. Turitsyn S K *Phys. Rev. E* **47** R796 (1993)
24. Flytzanis N, Savin A V, Zolotaryuk Y *Phys. Lett. A* **193** 148 (1994)
25. Peyrard M, Bishop A R *Phys. Rev. Lett.* **62** 2755 (1989)
26. Peyrard M et al. *Physica D* **68** 104 (1993)
27. Dauxois T, Peyrard M, Bishop A R *Phys. Rev. E* **47** R44 (1993)
28. Yakushevich L V *Nonlinear Physics of DNA* (New York: Wiley, 1998)
29. Netrebko A V et al. *Izv. Vyssh. Uchebn. Zaved. Priklad. Nelin. Dinamika* **2** (3) 26 (1994)
30. Romanovsky Yu M *Lecture Notes in Physics* **484** 140 (1997)
31. Zolotaryuk A V, Christiansen P L, Savin A V *Phys. Rev. E* **54** 3881 (1996)
32. Christiansen P L, Zolotaryuk A V, Savin A V *Phys. Rev. E* **56** 877 (1997)
33. Flytzanis N, Pnevmatikos St, Remoissent M *J. Phys. C* **18** 4603 (1985)
34. Flytzanis N, Pnevmatikos St, Peyrard M *J. Phys. A* **22** 783 (1989)
35. Cadet S *Phys. Lett. A* **121** 77 (1987)
36. Manevich L I et al. *Khim. Fiz.* **9** 552 (1990)
37. Manevich L I, Ryapusov S V *Fiz. Tverd. Tela* (Leningrad) **34** 1554 (1992) [*Sov. Phys. Solid State* **34** 826 (1992)]
38. Atoji M, Lipscomb W N *Acta Crystallogr.* **7** 173 (1954)
39. Ghelfenmstein M, Szwarc H *Mol. Cryst. Liq. Cryst.* **14** 273 (1971)
40. Anderson A, Torrie B H, Tse W S *J. Raman Spectroscopy* **10** 148 (1981)
41. Eilbeck J C, Flesch R *Phys. Lett. A* **194** 200 (1990)
42. Duncan D B et al. *Physica D* **68** 1 (1993)
43. Kirkwood J G *J. Chem. Phys.* **7** 506 (1939)
44. Zarkhin L S et al. *Usp. Khim.* **58** 644 (1989) [*Sov. Chem. Usp.* **00** 000 (1989)]

45. Manevitch L I, Zarkhin L S, Enikolopyan N S *J. Appl. Polymer Sci.* **39** 2245 (1990)
46. Manevich L I, Savin A V *Vysokomol. Soedin. A* **38** 1209 (1996)
47. Manevitch L I, Savin A V *Phys. Rev. E* **55** 4713 (1997)
48. Sumpter B G et al. *Adv. Polymer Sci.* **116** 29 (1994)
49. Zhang F *Phys. Rev. E* **56** 6077 (1997)
50. Christiansen P L, Savin A V, Zolotaryuk A V *J. Comp. Phys.* **134** 108 (1997)
51. Nagle J F, Morowitz H J *Proc. Natl. Acad. Sci. USA* **75** 298 (1978)
52. Nagle J F, Mille M, Morowitz H J *J. Chem. Phys.* **72** 3959 (1980)
53. Nagle J F, Tristram-Nagle S *J. Membrane Biol.* **74** 1 (1983)
54. Stogryn D E, Stogryn A P *Mol. Phys.* **11** 371 (1966)
55. Cournoyer M E, Jorgensen W L *Mol. Phys.* **51** 119 (1984)
56. Nemukhin A V *Zh. Fiz. Khim.* **66** 4 (1992)